Title

Interfacial Electron Transfer of Ferrocene Immobilized onto Indium Tin Oxide through Covalent and Noncovalent Interactions

Permalink

https://escholarship.org/uc/item/3b5515k4

Journal

ACS Applied Materials & Interfaces, 10(15)

ISSN

1944-8244

Authors

Hanna, Caitlin M

Sanborn, Christopher D

Ardo, Shane

et al.

Publication Date

2018-04-18

DOI

10.1021/acsami.8b01219

Supplemental Material

https://escholarship.org/uc/item/3b5515k4#supplemental

ACS APPLIED MATERIALS & INTERFACES

Research Article

Cite This: ACS Appl. Mater. Interfaces 2018, 10, 13211−13217

www.acsami.org

Interfacial Electron Transfer of Ferrocene Immobilized onto Indium Tin Oxide through Covalent and Noncovalent Interactions

Caitlin M. Hanna,[†] Christopher D. Sanborn,[†] Shane Ardo,[†,‡] and Jenny Y. Yang*,[†]

[†]Department of Chemistry and [‡]Department of Chemical Engineering and Materials Science, University of California, Irvine, California 92697, United States

Supporting Information

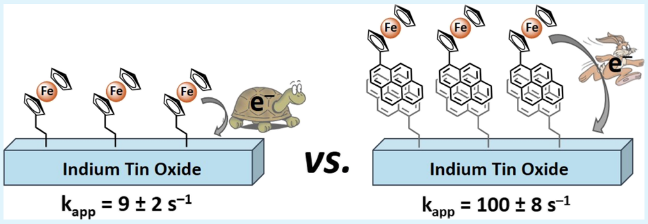

ABSTRACT: The immobilization of molecular species onto electrodes presents a direct route to modifying surface properties with molecular fidelity. Conventional methods include direct covalent attachment and physisorption of pyrene-appended molecular compounds to electrodes with aromatic character through $\pi-\pi$ interactions. A recently reported hybrid approach extends the synthetic flexibility of the latter to a broader range of electrode materials. We report an application of this approach to immobilization of pyrene-appended ferrocene onto pyrene-functionalized indium tin oxide (ITO). The modified ITO surfaces were characterized using X-ray photoelectron spectroscopy, fluorescence spectroscopy, and electrochemical techniques. An electron-transfer rate constant (k_{app}) of 100 ± 8 s^{-1} was measured between the electrode and immobilized ferrocene using electrochemical methods. For comparison, a ferrocene-modified electrode using conventional covalent attachment of vinylferrocene was also prepared, and k_{app} was measured to be 9 ± 2 s^{-1}.

KEYWORDS: *noncovalent immobilization, interfacial electron transfer, indium tin oxide, pyrene, chemically modified electrode*

■ INTRODUCTION

Integration of molecular species with surfaces to generate chemically modified electrodes (CMEs) provides a practical route for the synthesis of materials with molecular specificity. The development of new CMEs requires an attachment methodology that is both synthetically accessible and promotes interfacial charge transfer. Traditionally, molecular species have been immobilized onto electrodes using two different methods (Scheme 1, covalent and noncovalent attachment). The first utilizes covalent bonds between the molecule and the electrode.[1,2] This method requires that the molecular species is compatible with the functional groups (i.e., Grignard,[3,4] thiol,[5,6] diamine,[7−9] or vinyl)[5,10,11] used to forge covalent bonds to the surface. The second approach is to affix the molecular species with inert pyrene functionalities and utilize $\pi-\pi$ interactions for physisorption onto graphitic electrodes such as highly oriented pyrolytic graphite (HOPG), carbon nanotubes, or graphene.[7,12−17] Covalent attachment limits the scope of molecular species that can be immobilized onto surfaces, whereas noncovalent attachment is restricted to electrodes with a graphitic character.

We recently reported a synthetically facile approach to molecular immobilization that broadens the scope of CMEs (Scheme 1, bottom, hybrid attachment). Pyrene molecules are easily functionalized and stable to a large range of reactive functional groups for covalent attachment to nongraphitic surfaces. Pyrene-appended redox-active molecules are then physisorbed onto these surfaces through noncovalent interactions. We previously applied this method to the noncovalent immobilization of 1-pyrenylferrocene to gold.[18]

In this study, we demonstrate the generality of our approach by immobilizing 1-pyrenylferrocene to pyrene-modified indium tin oxide (ITO) electrodes and measure the rate constant of electron transfer through the interface. Ferrocene was selected because of its near-ideal redox properties. Additionally, it is relatively inert and easily functionalized for direct covalent attachment, permitting a comparison of interfacial properties between the two methods of electrode modification. Our measurements indicate that electron transfer through the pyrene−pyrene interface has a greater electron transfer rate constant compared with covalent ferrocene attachment and is comparable to published values for electron transfer through pyrene−graphitic interfaces.[19] Our results establish that the modular hybrid method of accessing new CMEs through noncovalent interactions has comparable or improved interfacial electron-transfer kinetics relative to the established methods.

■ EXPERIMENTAL DETAILS

General Procedures. All reactions and manipulations were performed under an atmosphere of N_2 unless otherwise specified. Solvents were dried and degassed by sparging with argon and dried by passing through columns of neutral alumina or molecular sieves in an

Received: January 23, 2018
Accepted: March 19, 2018
Published: April 6, 2018

DOI: 10.1021/acsami.8b01219
ACS Appl. Mater. Interfaces 2018, 10, 13211−13217

Scheme 1. Overview of Methods for Molecular Attachment to Electrode Surfaces

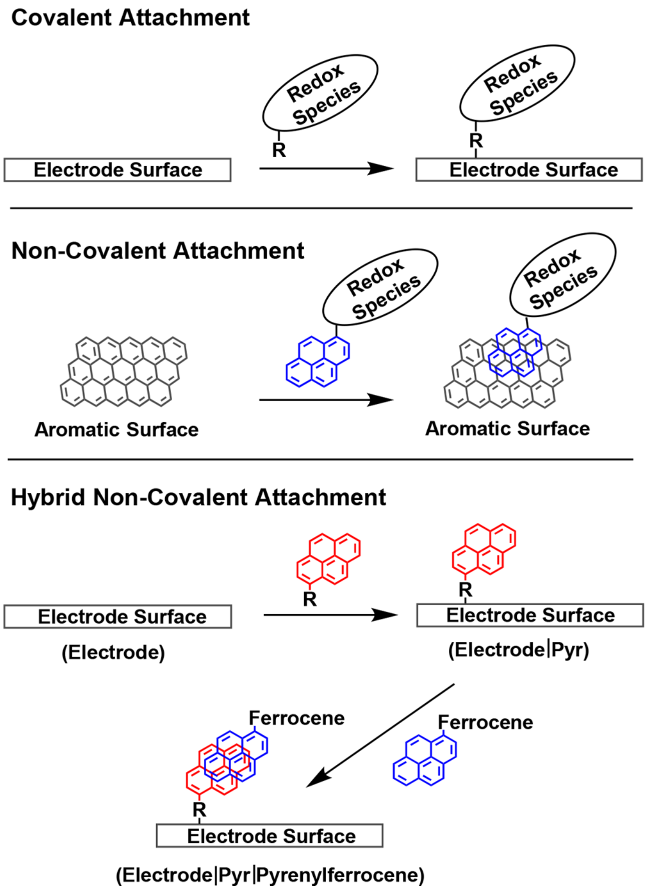

inert atmosphere. ITO on boro-aluminosilicate glass with a thickness of 0.5 mm and a sheet resistance of 5−15 Ω/sq was purchased from Delta Technologies. 1-Pyrenylferrocene[18] and 1-vinylpyrene[20] were prepared using previously published procedures. All other materials and reagents were purchased from commercial suppliers and used without purification (Aldrich and Fisher).

Physical Methods. X-ray photoelectron spectra were acquired with a Kratos Analytical AXIS Supra spectrometer utilizing monochromatic Al Kα radiation (1486.7 eV, 250 W) under ultrahigh vacuum conditions (~10^{-9} Torr). Survey spectra were collected with a pass energy of 160 eV, and high-resolution scans were performed with a pass energy of 20 eV. The binding energies were referred to the C 1s signal at 285 eV. Spectral data were analyzed using computer-aided surface analysis for X-ray photoelectron spectroscopy. Shirley or linear backgrounds and Gaussian−Lorentzian lineshapes were used to model peaks.

Two-photon fluorescence spectral images of the functionalized ITO surface were obtained using a modified Olympus FV1000 with an IX81 (Olympus Corporation) confocal laser scanning microscope and a water objective with a 1.2 numerical aperture. Samples were illuminated with a titanium:sapphire laser (Coherent Inc.) operating at a wavelength of 714 nm. For fluorescence spectral image acquisition, the emission signal was delivered to a Shamrock SR-303i spectrograph (Andor Technology) equipped with 512-channel ultrafast iXon Ultra EMCCD (Andor Technology). Spectra were acquired with an exposure time of 37 μs and corrected with a spectral response curve of the system calibrated using a tungsten lamp. For a detailed description of the setup and experimental conditions see ref 21.

Electrochemical Experiments. Electrochemical experiments were carried out in either 100 mM aqueous KCl solutions or 100 mM NBu_4PF_6 solutions in anhydrous organic solvents. Three electrode cyclic voltammetry experiments were performed with a Pine WaveDriver 10 potentiostat using AfterMath software. A 1 mm diameter glassy carbon disk working electrode was used for all homogeneous electrochemical experiments. A glassy carbon rod was used as the auxiliary electrode in all electrochemical experiments. Aqueous potentials are referenced to a saturated calomel electrode (SCE) and nonaqueous potentials are referenced to $Cp_2Fe^{+/0}$ (Cp = cyclopentadienyl), using $Cp_2Co^{+/0}$ (−1.33 V vs $Cp_2Fe^{+/0}$) or $Cp_2^*Fe^{+/0}$ (−0.48 V vs $Cp_2Fe^{+/0}$) (Cp* = pentamethylcyclopentadienyl) as the internal standard because of the overlap of analyte redox couples with the ferrocene redox couple.[22] All reported peak current densities are corrected for capacitive currents using AfterMath software.

Substrate Modification. ITO electrodes were cleaned by immersing the samples in a series of solvents at 50 °C for 10 min each. The order of solvents was as follows: trichloroethylene, acetone, and methanol. The electrodes were rinsed with H_2O and dried under a stream of N_2 after each solvent. Electrodes were functionalized immediately after cleaning. Clean ITO samples were placed in vial, ITO side facing up, and immersed in a 1 mM solution of 1-vinylpyrene in anhydrous toluene. The solution was heated to 80 °C for 24 h. The samples were removed from the vial, rinsed with anhydrous toluene and CH_2Cl_2, and dried under a stream of N_2. ITO|Pyr samples were placed in a 1 mM solution of 1-pyrenylferrocene in anhydrous CH_2Cl_2 for 12 h. The samples were removed from the solution, rinsed with anhydrous CH_3CN to remove loosely bound species, and dried to give ITO|Pyr|pyrenylferrocene. ITO|vinylferrocene samples were prepared by immersing a clean ITO sample in a 1 mM solution of vinylferrocene in $(n\text{Bu})_2O$ at 80 °C for 24 h. The samples were then rinsed with $(n\text{Bu})_2O$ and dried under N_2.

■ RESULTS AND DISCUSSION

Modification of ITO Surfaces. 1-Vinylpyrene[20] and 1-pyrenylferrocene[18] were prepared using previously published procedures. Covalent attachment of pyrene and ferrocene to ITO was achieved by immersing clean ITO samples in toluene solutions of 1-vinylpyrene or $(n\text{Bu})_2O$ solutions of vinylferrocene at 80 °C for 24 h to yield pyrene-modified ITO (ITO|Pyr) and ferrocene-modified ITO (ITO|vinylferrocene). Vinyl functionalities are commonly grafted onto metal oxide surfaces via cathodic electropolymerization or exposure to UV light.[11,23−25] Recent studies on the attachment of alkenes and alkynes to hydroxyl-terminated surfaces using heat found that a thermal approach leads to covalently bound monolayers as opposed to polymerized multilayers.[26] A thermal attachment approach was therefore chosen for this study to avoid multilayer formation of the covalently linked species. Finally, 1-pyrenylferrocene was physisorbed to the ITO|Pyr surface by soaking ITO|Pyr samples in a 1 mM CH_2Cl_2 solution of the metal complex for 12 h followed by rinsing with CH_3CN, a solvent in which the free complex is soluble, resulting in ITO|Pyr noncovalently modified with 1-pyrenylferrocene (ITO|Pyr|pyrenylferrocene).

Surface Characterization of Noncovalently Modified ITO. *Fluorescence Spectroscopy.* Fluorescence emission spectroscopy was used to confirm the attachment of 1-vinylpyrene to the ITO surface and give insights into the noncovalent interactions between pyrene molecules on the surface. The fluorescence emission spectrum of ITO|Pyr, displayed in black in Figure 1, exhibits an emission band with a maximum at 440 nm. The broad and featureless emission of ITO|Pyr is attributed to the face-to-face excimer of pyrene which is commonly observed in the emission spectra of bipyrenyl compounds and highly concentrated pyrene solutions.[27,28] These results agree well with literature reports of the fluorescence of pyrene and 1-vinylpyrene adsorbed on oxide supports,[25,29] confirming the presence of pyrene on the

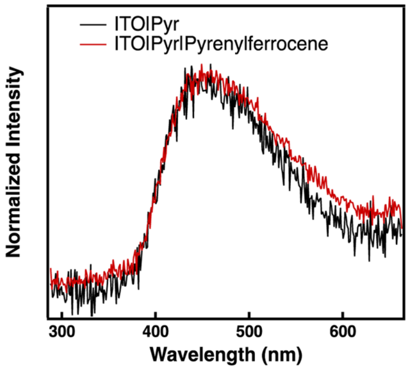

Figure 1. Two-photon fluorescence emission spectra of ITO|Pyr (black trace) and ITO|Pyr|pyrenylferrocene (red trace).

surface and indicating that the pyrene molecules are oriented on the surface in a way that promotes face-to-face excimer formation upon excitation. The fluorescence emission spectrum of ITO|Pyr|pyrenylferrocene is shown in red in Figure 1; there are no significant differences between the emission spectrum of ITO|Pyr and ITO|Pyr|pyrenylferrocene. The lack of difference between the emission spectrum of ITO|Pyr|pyrenylferrocene compared with that of ITO|Pyr suggests that pyrene molecules are still oriented in a face-to-face manner but does not provide additional insights into the interaction between surface-bound pyrene and ferrocene-bound pyrene.

X-ray Photoelectron Spectroscopy. The XPS survey spectra of unmodified ITO, ITO|Pyr, and ITO|Pyr|pyrenylferrocene are shown in Figures S1−S3. All three spectra exhibit expected peaks from indium, tin, oxygen, and carbon. Upon functionalization of ITO with 1-vinylpyrene, there are no changes to the XPS spectrum other than an increase in the C 1s signal. This is expected because of the lack of XPS signatures present in 1-vinylpyrene. Physisorption of 1-pyrenylferrocene onto the ITO|Pyr surface results in the appearance of an Fe $2p_{3/2}$ peak at 708 eV and an Fe $2p_{1/2}$ peak at 721 eV (Figure 2), confirming the presence of 1-pyrenylferrocene on the surface. These peaks exhibit a 2:1 branching ratio expected for 2p photoelectrons. The peaks at 704 and 717 eV are attributed to In $3p_{1/2}$ and Sn $3p_{3/2}$, respectively. The XPS spectra of the Fe 2p region of unmodified ITO and ITO|Pyr exhibit peaks attributed to In $3p_{1/2}$ and Sn $3p_{3/2}$ but do not display any Fe 2p features (Figures S4 and S5). These results confirm the presence of 1-pyrenylferrocene on the ITO|Pyr|pyrenylferrocene surface.

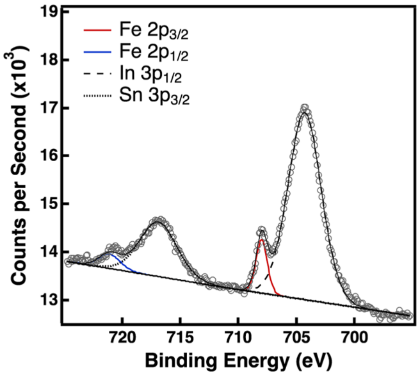

Figure 2. High-resolution XPS spectrum of the Fe 2p region of ITO|Pyr|pyrenylferrocene.

Electrochemical Characterization. *Cyclic Voltammetry of Noncovalently Modified ITO Electrodes.* Cyclic voltammetry of ITO|Pyr|pyrenylferrocene was performed to probe electron transfer between the ITO electrode and surface-bound ferrocene. The cyclic voltammogram (CV) of ITO|Pyr|pyrenylferrocene in 100 mM aqueous solution of KCl displays a reversible redox couple at 0.46 V versus SCE with a full width at half-maximum (fwhm) of 0.16 V and peak separation of 0.04 V (Figure 3). The fwhm is greater than the ideal value of 0.09 V, suggesting the electrostatic interaction between neighboring ferrocene complexes.[30,31] The cathodic to anodic peak separation also deviated from an ideal value of 0 V, which again is likely due to the electrostatic interaction between neighboring ferrocene molecules.[31,32] The $E_{1/2}$ value observed is consistent with that in the literature reports of surface-bound ferrocene.[18,32] The insolubility of 1-pyrenylferrocene in water prevents homogeneous studies under identical conditions, but studies in CH_3CN display a reversible redox couple at 0.05 V versus $Cp_2Fe^{+/0}$ (Figure S6).

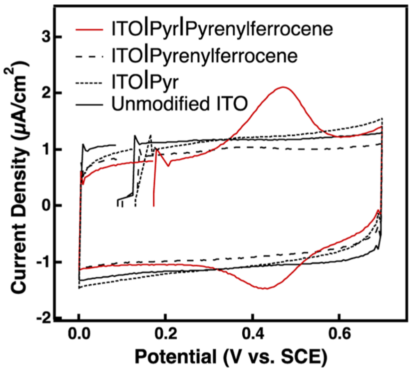

Figure 3. Cyclic voltammetry of ITO|Pyr|pyrenylferrocene and control experiments performed in 100 mM aqueous KCl at 100 mV/s.

Consecutive CVs of ITO|Pyr|pyrenylferrocene are displayed in Figure S8. There is negligible change in the area under the anodic curve with up to 25 scans, indicating that physisorption of 1-pyrenylferrocene on the ITO|Pyr surface is stable throughout oxidation/reduction cycles under aqueous conditions. To analyze the importance of the surface-bound pyrene in immobilization of 1-pyrenylferrocene, an unmodified ITO sample was soaked in 1-pyrenylferrocene under the same conditions as the previously described attachment procedure. The CV of this sample does not display the $Cp_2Fe^{+/0}$ couple, indicating that the pyrene layer is necessary for the successful retention of 1-pyrenylferrocene on the surface under aqueous conditions. Furthermore, no redox events are observed between 0.00 and 0.70 V versus SCE for unmodified ITO or ITO|Pyr (Figure 3).

Variable scan rate CVs for ITO|Pyr|pyrenylferrocene and the corresponding peak current density versus scan rate plot is shown in Figure 4. Peak current densities vary linearly with the scan rate, diagnostic of a surface-bound redox species. Integration of the anodic faradaic current was used to calculate the electrochemically active coverage of 1-pyrenylferrocene on the ITO|Pyr surface. The average electrochemically active surface coverage across all samples was calculated to be 5 pmol/cm^2. Efforts to increase the coverage by extending the sample immersion time and using highly concentrated solutions of 1-pyrenylferrocene during sample preparation led to the same amount of electroactive species.

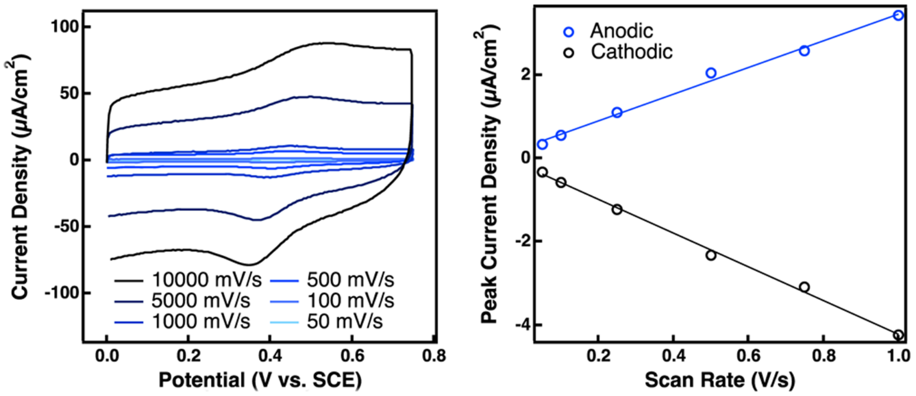

Figure 4. Variable scan rate cyclic voltammetry of ITO|Pyr|pyrenylferrocene performed in 100 mM aqueous KCl (left) and the corresponding current density vs scan rate plot (right).

Solvent Effects on the Stability of Noncovalently Modified ITO Electrodes. Solvophobic effects are known to be important factors in the stability of $\pi-\pi$ interactions.[33] In order to probe the contribution of hydrophobicity toward the stability of the ITO|Pyr|pyrenylferrocene system, cyclic voltammetry was performed in CH_3CN, a solvent in which 1-pyrenylferrocene is soluble. The CVs of ITO|Pyr|pyrenylferrocene in CH_3CN are displayed in Figure S9. In the first scan, a reversible redox couple attributed to surface-bound ferrocene is observed. Integration of the anodic faradaic current was used to calculate an electrochemically active surface coverage of 3 pmol/cm^2. The electrochemically active surface coverage decreases to 1 pmol/cm^2 in the second scan and finally zero in the third scan. The decrease in the surface coverage indicates that 1-pyrenylferrocene desorbs from the surface during the course of three CV experiments in nonaqueous solvents, highlighting the importance of solvophobic effects in stabilizing the ITO|Pyr|pyrenylferrocene system.

Electron-Transfer Kinetics. *Noncovalently Modified ITO Electrodes.* The rate of electron transfer between the electrode and immobilized 1-pyrenylferrocene was determined using the Butler–Volmer approach.[34] The separation of anodic and cathodic peaks with the increasing scan rate observed in Figure 4 can be used to calculate the apparent rate constant of the system according to the Laviron formalism[34] using the following set of equations

$$E_{p,c} = E^{\circ\prime} - \frac{2.3RT}{\alpha nF}\log\left[\frac{\alpha nFv}{RTk_{app}}\right] \tag{1}$$

$$E_{p,a} = E^{\circ\prime} - \frac{2.3RT}{(1-\alpha)nF}\log\left[\frac{(1-\alpha)nFv}{RTk_{app}}\right] \tag{2}$$

where $E_{p,a}$ is the potential of the anodic peak, $E_{p,c}$ is the potential of the cathodic peak, $E^{\circ\prime}$ is the formal potential calculated by averaging the anodic and cathodic potentials at slow scan rates, v is the scan rate, α is the electron-transfer coefficient, k_{app} is the apparent rate constant, R is the ideal gas constant, T is the absolute temperature, F is the Faraday constant, and n is the number of electrons transferred. Electron-transfer parameters (v_a, v_c, α, and k_{app}) are determined by plotting $E_p - E^{\circ\prime}$ against the log of the scan rate (trumpet plot). The critical scan rates, v_a and v_c, are determined by extrapolating the linear portions of the plot where $(E_p - E^{\circ\prime}) >$ 100 mV to 0 and α is obtained from the slopes of the linear fits. k_{app} is calculated using v_a, v_c, and α and reported as the average of $k_{app,c}$ and $k_{app,a}$ across three individually prepared samples (see the Supporting Information for a detailed sample calculation).

The trumpet plot for the ITO|Pyr|pyrenylferrocene system is displayed in Figure 5. Using the slopes of the linear portions of the trumpet plot, the electron transfer coefficients, α and $(1 - \alpha)$, were calculated to be 0.44 and 0.26, respectively. The transfer coefficients calculated for the ITO|Pyr|pyrenylferrocene system in water deviate from 0.5 and do not have a unity sum, both of which would be expected for an outer-sphere one electron redox process. Similar deviations are exhibited in the literature reports of surface-bound ferrocene, where α and $(1 - \alpha)$ are 0.23 and 0.24, respectively.[35] These low transfer coefficients with a nonunity sum suggest a film structure with exposed ITO sites.[35,36] k_{app} for the ITO|Pyr|pyrenylferrocene system was determined to be 100 ± 8 s^{-1} (more details on the calculation can be found in the Supporting Information). This rate constant is two orders of magnitude greater than the electron-transfer rate constant reported for ferrocene dicarboxylic acid adsorbed on ITO surfaces via hydrogen bonding interactions, despite the longer linker length in ITO|Pyr|pyrenylferrocene.[37] It is possible that the hydrophobicity of the pyrene groups is causing ferrocene to lie flat on the electrode during aqueous chemistry, decreasing the distance between ITO and noncovalently bound ferrocene. However, a deeper understanding of the electron transfer pathway in ITO|Pyr|

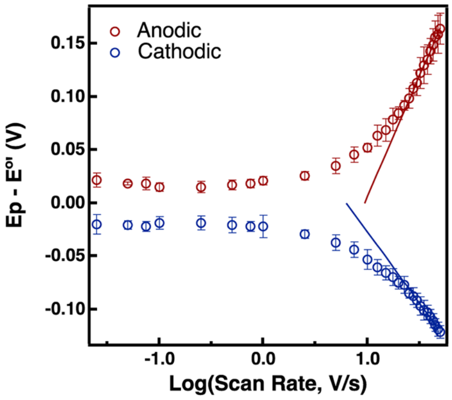

Figure 5. Trumpet plot of ITO|Pyr|pyrenylferrocene in 100 mM aqueous KCl.

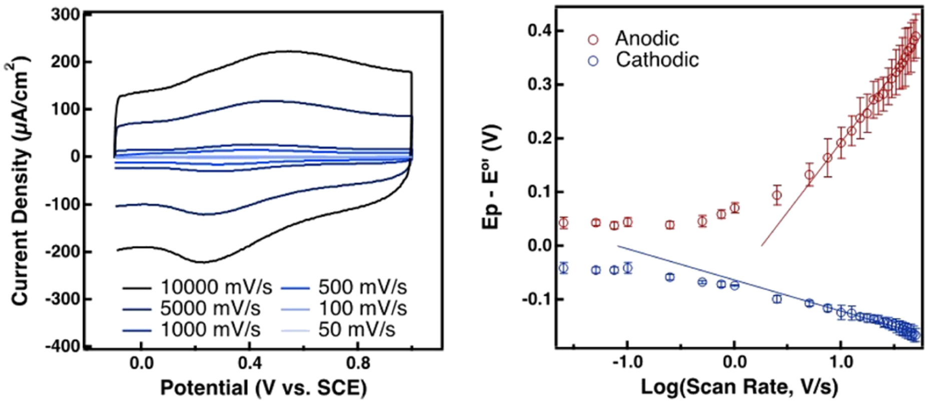

Figure 6. Variable scan rate cyclic voltammetry of ITO|vinylferrocene performed in 100 mM aqueous KCl (left) and the corresponding trumpet plot (right).

pyrenylferrocene is necessary to fully understand the basis for the enhanced rate of electron transfer using this approach.

Covalently Modified ITO Electrodes. Vinylferrocene was immobilized onto ITO by direct covalent attachment (ITO|vinylferrocene) to compare the electron-transfer kinetics with noncovalently bound ferrocene. The high-resolution XPS spectrum of the Fe 2p region of ITO|vinylferrocene (Figure S10) displays peaks attributed to Fe 2p photoelectrons, confirming the presence of vinylferrocene on the surface. Homogeneous cyclic voltammetry of vinylferrocene performed in CH_3CN is shown in Figure S11; a reversible redox couple is seen at −0.04 V versus $Cp_2Fe^{+/0}$. The CV of ITO|vinylferrocene displays a reversible redox couple at 0.34 V versus SCE with an fwhm of 0.32 V. As seen in the CV of noncovalently bound ferrocene, the fwhm is greater than the ideal value of 0.09 V, suggesting electrostatic interactions between neighboring ferrocene groups.[30,31] The deviation of the fwhm from ideality of the ITO|vinylferrocene system is greater than that of the ITO|Pyr|pyrenylferrocene system, indicating greater interaction between the ferrocene centers in the covalent system.[34] Integration of the anodic faradaic current was used to calculate the electrochemically active coverage of vinylferrocene on the ITO surface. The average electrochemically active surface coverage across all samples was calculated to be 30 pmol/cm^2, six times greater than that of noncovalently bound 1-pyrenylferrocene. The variable scan rate CVs of this system (Figure 6) and the corresponding current density versus scan rate plot (Figure S13) display a linear relationship between current density and scan rate, confirming that ferrocene is bound to the surface.

The anodic and cathodic peaks of the ITO|vinylferrocene CVs separate with increasing scan rate, as seen in the ITO|Pyr|pyrenylferrocene system. The trumpet plot for the ITO|vinylferrocene system is displayed in Figure 6. The transfer coefficients, α and $(1 - \alpha)$, were calculated to be 0.71 and 0.23, respectively. The increase in the transfer coefficient values and their near-unity sum compared with those of ITO|Pyr|pyrenylferrocene suggest a film structure with fewer exposed ITO sites in the ITO|vinylferrocene system, consistent with the increased electrochemically active ferrocene coverage exhibited in ITO|vinylferrocene.[35] The rate constant, k_{app}, was calculated to be 9 ± 2 s^{-1}. These results indicate that the apparent rate of electron transfer of the noncovalent ITO|Pyr|pyrenylferrocene system is greater than that of the covalent ITO|vinylferrocene system.

A notable difference between the trumpet plots of ITO|Pyr|pyrenylferrocene and ITO|vinylferrocene is the symmetry of the anodic and cathodic portions of the plots. According to initial theoretical investigations by Laviron, the asymmetry exhibited in the trumpet plot of ITO|vinylferrocene is a consequence of transfer coefficient values exceeding 0.5.[34] In reports of 2-aza[3]ferrocenophane covalently attached to gold, similar asymmetry is seen when electrochemistry is performed in acidic media, which is attributed to an imbalance of the mass transport of ions in the anodic and cathodic processes.[38] On the basis of the increased electrochemically active ferrocene coverage of ITO|vinylferrocene relative to that of ITO|Pyr|pyrenylferrocene, imbalances of the mass transport of ions may be affecting the ITO|vinylferrocene system more significantly than the ITO|Pyr|pyrenylferrocene system, resulting in a more asymmetric trumpet plot.

Electron Transfer through Coventional π–π Interfaces. Our attempts to physisorb 1-pyrenylferrocene onto an HOPG electrode did not provide sufficiently stable immobilization to conduct electron-transfer measurements. A recent study on the immobilization of pyrene-appended ruthenium complexes onto HOPG, where rate constants were calculated to be 64 and 110 s^{-1} for complexes functionalized with 8 and 4 pyrene molecules per ruthenium, respectively, found that the kinetic stability of adsorption on HOPG increased with the increasing number of pyrene groups on the complexes.[19] 1-Pyrenylferrocene may be desorbing from the HOPG surface because of the single pyrene moiety on the molecule. We hypothesize that 1-pyrenylferrocene remains stable on the ITO|Pyr surface because of the interaction of the single ferrocene-bound pyrene with multiple surface-bound pyrene groups. The fluorescence emission data of the ITO|Pyr surface indicate that the surface-bound pyrene groups are oriented close enough to one another to form face-to-face eximers upon excitation. As a result, each immobilized 1-pyrenylferrocene molecule may be stabilized by π–π interactions from multiple surface-bound pyrene groups.

■ CONCLUSION

Electrochemical analysis of the ITO|Pyr|pyrenylferrocene system reveals facile electron transfer between the ITO electrode and the surface-bound ferrocene. The electron-transfer studies of ITO|Pyr|pyrenylferrocene indicate it has comparable kinetics with noncovalent attachment of a pyrene appended molecule onto HOPG. Comparison of ITO|Pyr|pyrenylferrocene with ITO|vinylferrocene indicates that electron transfer for the noncovalent attachment system is 10 times faster than that for an analogous covalent attachment system. These results establish that our noncovalent attachment method provides a means for robust molecular attachment to surfaces with facile electron transfer between the electrode and the immobilized species. The electron transfer rate constant required to keep up with the solar flux at a single site 10% catalyst coverage surface is 10 s^{-1}.[39] Thus, electron transfer of the ITO|Pyr|pyrenylferrocene system (100 ± 8 s^{-1}) is kinetically viable for solar-driven photoelectrochemical applications.

The distance between the electrode and the redox-active species[40] and the extent of π-conjugation of the linker attaching the redox species to the electrode[41] are potential factors influencing the kinetics of electron transfer. Further investigation of the electron-transfer pathway in ITO|Pyr|pyrenylferrocene and ITO|vinylferrocene is necessary to determine the source of enhanced electron-transfer kinetics exhibited by the attachment systems that utilize $\pi-\pi$ interactions. The possibility of polymerization of the vinyl functionalities used to covalently attach pyrene and ferrocene to the ITO surfaces should also be considered in evaluating electron-transfer kinetics of the ITO|Pyr|pyrenylferrocene and ITO|vinylferrocene systems. Although previous studies suggest that the thermal attachment approach leads to monolayer formation rather than polymerization,[26] we were unable to confirm this experimentally on our surfaces. Some polymerization would likely affect the rate of electron transfer between the ITO and surface-bound ferrocene.

Sequential CVs highlight the stability of the system in aqueous conditions and reduced stability in solvents in which 1-pyrenylferrocene is soluble. These results suggest that our noncovalent attachment method is most useful for attaching molecules that are insoluble in the solvent of interest. Efforts geared toward strengthening the $\pi-\pi$ interactions between the surface-bound aromatic molecule and complex-bound pyrene to improve the stability over a range of conditions are currently being pursued.

■ ASSOCIATED CONTENT

Ⓢ Supporting Information

The Supporting Information is available free of charge on the ACS Publications website at DOI: 10.1021/acsami.8b01219.

XPS spectra, additional CV electrochemical analysis, and sample calculations (PDF)

■ AUTHOR INFORMATION

Corresponding Author

*E-mail: j.yang@uci.edu.

ORCID

Shane Ardo: 0000-0001-7162-6826

Jenny Y. Yang: 0000-0002-9680-8260

Notes

The authors declare no competing financial interest.

■ ACKNOWLEDGMENTS

This study was supported by the Hellman Faculty Fellows Fund, the School of Physical Sciences at UC Irvine, and the U. S. Department of Energy, Office of Science, Office of Basic Energy Sciences under award number DE-SC0012150. XPS work was performed at the UC Irvine Materials Research Institute (IMRI) using instrumentation funded in part by the National Science Foundation Major Research Instrumentation Program under grant no. CHE-1338173. Two-photon spectral imaging experiments reported in this paper were performed at the Laboratory for Fluorescence Dynamics (LFD) at the University of California, Irvine (UCI). The LFD is supported jointly by the National Institutes of Health (2P41GM103540) and UCI.

■ REFERENCES

(1) Vericat, C.; Vela, M. E.; Corthey, G.; Pensa, E.; Cortés, E.; Fonticelli, M. H.; Ibañez, F.; Benitez, G. E.; Carro, P.; Salvarezza, R. C. *RSC Adv.* **2014**, *4*, 27730−27754.

(2) Casalini, S.; Bortolotti, C. A.; Leonardi, F.; Biscarini, F. *Chem. Soc. Rev.* **2017**, *46*, 40−71.

(3) Brown, E. S.; Peczonczyk, S. L.; Wang, Z.; Maldonado, S. *J. Phys. Chem. C* **2014**, *118*, 11593−11600.

(4) Mukherjee, J.; Peczonczyk, S.; Maldonado, S. *Langmuir* **2010**, *26*, 10890−10896.

(5) Richards, D.; Zemlyanov, D.; Ivanisevic, A. *Langmuir* **2010**, *26*, 8141−8146.

(6) Cuypers, D.; Fleischmann, C.; van Dorp, D. H.; Brizzi, S.; Tallarida, M.; Müller, M.; Hönicke, P.; Billen, A.; Chintala, R.; Conard, T.; Schmeißer, D.; Vandervorst, W.; Van Elshocht, S.; Armini, S.; De Gendt, S.; Adelmann, C. *Chem. Mater.* **2016**, *28*, 5689−5701.

(7) Oh, S.; Gallagher, J. R.; Miller, J. T.; Surendranath, Y. *J. Am. Chem. Soc.* **2016**, *138*, 1820−1823.

(8) Jackson, M. N.; Oh, S.; Kaminsky, C. J.; Chu, S. B.; Zhang, G.; Miller, J. T.; Surendranath, Y. *J. Am. Chem. Soc.* **2018**, *140*, 1004−1010.

(9) Fukushima, T.; Drisdell, W.; Yano, J.; Surendranath, Y. *J. Am. Chem. Soc.* **2015**, *137*, 10926−10929.

(10) Beiler, A. M.; Khusnutdinova, D.; Jacob, S. I.; Moore, G. F. *ACS Appl. Mater. Interfaces* **2016**, *8*, 10038−10047.

(11) Wadsworth, B. L.; Beiler, A. M.; Khusnutdinova, D.; Jacob, S. I.; Moore, G. F. *ACS Catal.* **2016**, *6*, 8048−8057.

(12) Lei, H.; Liu, C.; Wang, Z.; Zhang, Z.; Zhang, M.; Chang, X.; Zhang, W.; Cao, R. *ACS Catal.* **2016**, *6*, 6429−6437.

(13) Creus, J.; Matheu, R.; Peñafiel, I.; Moonshiram, D.; Blondeau, P.; Benet-Buchholz, J.; García-Antón, J.; Sala, X.; Godard, C.; Llobet, A. *Angew. Chem., Int. Ed.* **2016**, *55*, 15382−15386.

(14) Li, F.; Zhang, B.; Li, X.; Jiang, Y.; Chen, L.; Li, Y.; Sun, L. *Angew. Chem., Int. Ed.* **2011**, *50*, 12276−12279.

(15) Tran, P. D.; Le Goff, A.; Heidkamp, J.; Jousselme, B.; Guillet, N.; Palacin, S.; Dau, H.; Fontecave, M.; Artero, V. *Angew. Chem., Int. Ed.* **2011**, *50*, 1371−1374.

(16) Blakemore, J. D.; Gupta, A.; Warren, J. J.; Brunschwig, B. S.; Gray, H. B. *J. Am. Chem. Soc.* **2013**, *135*, 18288−18291.

(17) Maurin, A.; Robert, M. *J. Am. Chem. Soc.* **2016**, *138*, 2492−2495.

(18) Lydon, B. R.; Germann, A.; Yang, J. Y. *Inorg. Chem. Front.* **2016**, *3*, 836−841.

(19) Kohmoto, M.; Ozawa, H.; Yang, L.; Hagio, T.; Matsunaga, M.; Haga, M.-a. *Langmuir* **2016**, *32*, 4141−4152.

(20) Albagli, D.; Bazan, G. C.; Schrock, R. R.; Wrighton, M. S. *J. Phys. Chem.* **1993**, *97*, 10211−10216.

(21) Chen, H.; Gratton, E.; Digman, M. A. *Microsc. Res. Tech.* **2015**, *78*, 283−293.

(22) Connelly, N. G.; Geiger, W. E. *Chem. Rev.* **1996**, *96*, 877−910.

(23) Pujari, S. P.; Scheres, L.; Marcelis, A. T. M.; Zuilhof, H. *Angew. Chem., Int. Ed.* **2014**, *53*, 6322−6356.

(24) Franking, R. A.; Landis, E. C.; Hamers, R. J. *Langmuir* **2009**, *25*, 10676−10684.

(25) Kamat, P. V.; Basheer, R.; Fox, M. A. *Macromolecules* **1985**, *18*, 1366−1371.

(26) Pujari, S. P.; Scheres, L.; van Lagen, B.; Zuilhof, H. *Langmuir* **2013**, *29*, 10393−10404.

(27) Zachariasse, K. A.; Duveneck, G.; Busse, R. *J. Am. Chem. Soc.* **1984**, *106*, 1045−1051.

(28) Nakagawa, K.; Numata, Y.; Ishino, H.; Tanaka, D.; Kobayashi, T.; Tokunaga, E. *J. Phys. Chem. A* **2013**, *117*, 11449−11455.

(29) Francis, C.; Lin, J.; Singer, L. A. *Chem. Phys. Lett.* **1983**, *94*, 162−167.

(30) Eckermann, A. L.; Feld, D. J.; Shaw, J. A.; Meade, T. J. *Coord. Chem. Rev.* **2010**, *254*, 1769−1802.

(31) Bard, A. J.; Faulkner, L. R. *Electrochemical Methods*, 2nd ed.; John Wiley & Sons, Inc., 2001.

(32) Chidsey, C. E. D.; Bertozzi, C. R.; Putvinski, T. M.; Mujsce, A. M. *J. Am. Chem. Soc.* **1990**, *112*, 4301−4306.

(33) Martinez, C. R.; Iverson, B. L. *Chem. Sci.* **2012**, *3*, 2191−2201.

(34) Laviron, E. *J. Electroanal. Chem.* **1979**, *100*, 263−270.

(35) Hong, H. G.; Mallouk, T. E. *Langmuir* **1991**, *7*, 2362−2369.

(36) Finklea, H. O.; Avery, S.; Lynch, M.; Furtsch, T. *Langmuir* **1987**, *3*, 409−413.

(37) Donley, C.; Dunphy, D.; Paine, D.; Carter, C.; Nebesny, K.; Lee, P.; Alloway, D.; Armstrong, N. R. *Langmuir* **2002**, *18*, 450−457.

(38) Horie, M.; Sakano, T.; Osakada, K. *J. Organomet. Chem.* **2006**, *691*, 5935−5945.

(39) Li, F.; Basile, V. M.; Rose, M. J. *Langmuir* **2015**, *31*, 7712−7716.

(40) Smalley, J. F.; Feldberg, S. W.; Chidsey, C. E. D.; Linford, M. R.; Newton, M. D.; Liu, Y.-P. *J. Phys. Chem.* **1995**, *99*, 13141−13149.

(41) Sachs, S. B.; Dudek, S. P.; Hsung, R. P.; Sita, L. R.; Smalley, J. F.; Newton, M. D.; Feldberg, S. W.; Chidsey, C. E. D. *J. Am. Chem. Soc.* **1997**, *119*, 10563−10564.

DOI: 10.1021/acsami.8b01219
ACS Appl. Mater. Interfaces 2018, 10, 13211−13217